Evaluation of eddy currents dependent on excitation pattern in design of pulse electromagnets

T. Takayanagi, M. Sugita, T. Ueno, K. Horino, A. Ono, K. Yamamoto, and M. Kinsho

***Abstract*—The evaluation of a new shift bump magnet for replacement of the J-PARC (Japan Proton Accelerator Research Complex) RCS (Rapid Cycling Synchrotron) confirmed that the measured magnetic field waveform was different from the excitation-current waveform. The reason for this is the eddy-current effect due to the fast trapezoidal excitation pattern of approximately 1.5 ms. The same result was confirmed by OPERA-3D. A high-precision injection-beam orbit that suppresses device radiation due to beam loss was necessary. Therefore, in the excitation waveform of the injection bump magnet, the variation range at the flat-top must be less than ±1.0 %. We evaluated the effectiveness of the dynamic-magnetic field analysis of OPERA-3D comparison with the measurement results. An agreement with a 0.06 % deviation in the magnetic field distribution, the effect of eddy currents on the magnetic field waveform, and the potential of the analysis software for system design were confirmed. We also calculated the amount of heat generated by the bump-magnet coil and the necessary measures for operation. Furthermore, we verified that probes can accurately evaluate the pulsed excitation waveforms.**

***Index Terms*—Accelerator magnets, Electromagnetic analysis, Eddy current, Magnetic field measurement, Probes**

I. Introduction

THE 3-GeV RCS (Rapid Cycling Synchrotron) at the J-PARC (Japan Proton Accelerator Research Complex) [1],[2] has successfully accelerated a high-power beam that is equivalent to 1-MW at 25 Hz repetition [3],[4]. On the other hand, a new problem of high residual dose around the beam-injection area became has been encountered. To realize continuous 1-MW operation, shielding is required to reduce the radiation exposure during maintenance work. A proposal to replace the existing bump magnets with a new and smaller one to provide space for shielding is being considered [5]-[7]. On the other hand, the high flatness, which was less than ±1.0 % relative to the magnetic field waveform, fixed the orbit of the injection beam [8], [9].

We compared the results of dynamic electromagnetic simulations, which were performed by OPERA-3D [10], using measurements of the new shift bump magnet. OPERA-3D can analyze a time-varying magnetic field such as eddy currents, steady AC, and transient currents. As a result, we found that the current-excitation and measured magnetic field waveforms differed due to the eddy currents. By checking the variation of the flat-top due to the eddy current effect, the optimized parameter waveform for the power supply can be obtained. In addition, the heat generation of the coil was calculated to identify the problems of the cooling system and to calculate the operating parameters.

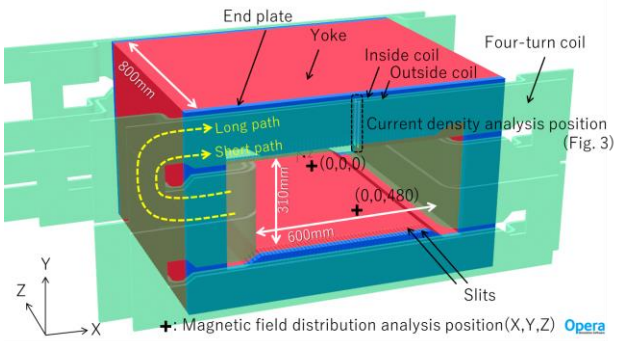

Fig. 1. New bump-magnet model of the OPERA-3D. The yoke is made of 0.2 mm electromagnetic laminated steel sheets with a length of 800 mm, and the endplates are 25 mm thick. The coil has four turns. The gap is 310 mm, and the distance between the inside surfaces of the coils is 600 mm. The 25 mm thick fringe section of the yoke and the end plates have 2 mm wide slits at 12 mm interval to prevent eddy currents.

II. Comparative Evaluation of the Analysis and Measurement Results

A. Dynamic magnetic field analysis using ELEKTRA by OPERA-3D

We used ELEKTRA [10] in OPERA-3D for the dynamic magnetic field analysis. The OPERA-3D model is shown in Fig. 1. The base-analysis electromagnet model was a new bump magnet intended for replacement. The structure of the electromagnet differed from the conventional ones in that it used an integrated yoke and a four-turn coil. The electromagnetic steel sheets used, the shape of the slit, and also the analysis of the OPERA-3D in the present study such as eddy current effect, skin effect, current drift, and waveform pattern dependence were based on the results of [5] and [7]. Magnetic field distributions B_y were calculated for X=Y=Z=0 mm at the center of the yoke and for X=Y=0 mm, and Z=480 mm at the fringe position immediately below the coil. We also analyzed the time variation in the current-density distribution at the inner and outer coil cross sections outside the yoke.

(Style: TAS First page footnote) Manuscript receipt and acceptance dates will be inserted here. Acknowledgment of support is placed in this paragraph as well. Consult the IEEE *Editorial Style Manual* for examples. This work was supported by the IEEE Council on Superconductivity under contract. ABCD-123456789. *(Corresponding author: Lance Cooley.)*

The authors are with J-PARC Accelerator Division in JAEA Energy Agency, Tokai, Ibaraki 319-1195, Japan (e-mail: tomohiro.takayanagi@j-parc.jp).

Color versions of one or more of the figures in this paper are available online at http://ieeexplore.ieee.org.

Digital Object Identifier will be inserted here upon acceptance.

This article has been accepted for publication in IEEE Transactions on Applied Superconductivity. This is the author's version which has not been fully edited and content may change prior to final publication. Citation information: DOI 10.1109/TASC.2022.3160152

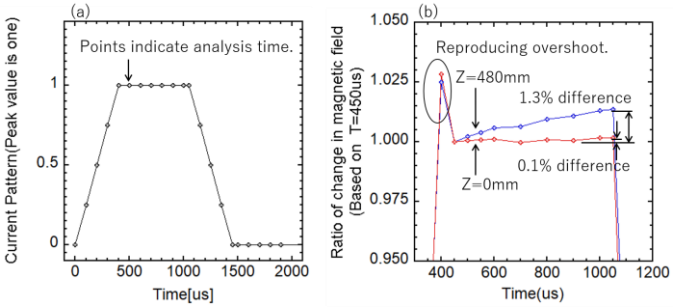

Fig. 2. Input waveform of OPERA-3D and the magnetic-field time variation results. (a) Input waveform. The rated current of 16 kA is set to one. The marks on the waveform indicate the analysis time. (b) Analysis result of the time variation in the magnetic field at X=Y=0 mm. Z=0 mm represents the center of the yoke. Z=480 mm indicates the fringe position.

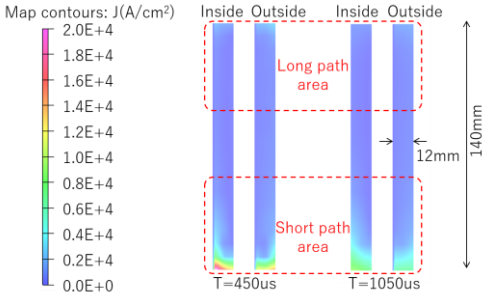

Fig. 3. Time variation in the current-density distribution in the coil, which shows the difference from immediately after the transition to the flat section. The current density was large in the shortest path at the bottom of the coil and gradually decreases. The width of the coil is 12 mm and the height is 140 mm.

The input waveform of the OPERA-3D and the results of the time variation in the magnetic field at the center and fringe positions are shown in Fig. 2. The marks on the waveform indicate the calculation time. In the trapezoidal waveform of 1450 μs, the results were calculated every 100 μs, whereas a shorter time of 50 μs was used in the transient part.

In the OPERA-3D results, the magnetic field at the center of the yoke varied with time by less than 0.1 %, whereas the magnetic field in the fringe region increased with time, indicating a change of 1.3 %. The magnetic flux that crossed the face of the electromagnetic steel sheet and edge plate was much higher than that in the central region where the flux was almost parallel to the steel face. The effect of the eddy current was larger at the peripheral fringe regions. However, the eddy currents gradually decayed along with the heat generated by the resistive component. The original magnetic field, which was partly cancelled by the eddy currents, was gradually restored, and the magnetic field appeared to increase.

The rapid change in the waveform approximately T=400 μs indicated an overshoot. OPERA-3D performs magnetic field analysis using an ideal excitation current waveform. At the timing when current waveform changes from slope to flat curve, overshoot then occurred in the simulation because no suppression elements/circuits were implemented to mitigate the sharp transient. However, in the real circuit, the voltage control loops to avoid such transients are provided, resulting in no overshoot. This point may cause uncertainty in the precise comparisons between the simulations and the measurements in the following sections. However, the eddy currents induced in the rising period of overshoot are estimated to be 2.5 % of those by the main field ramp between 0 and 400 μs, where the overshoot amplitude is 2.5 % of the main field. Moreover, in the subsequent falling period, the polarity of the induced voltages is changed to be negative, which cancels the effect in the preceding rising period. Therefore, it is considered that the effect of the overshoot is far less than 2.5 % of that by the main field and the following discussions will not be affected by the conditions whether there is an overshoot or not. Eddy currents during overshooting should be studied by detailed analysis.

The analysis results of the current-density distribution in the coil cross section are shown in Fig. 3. The current density after the transition from increasing to a flat shape at T=450 μs was high at the bottom of the coil where the current path was the shortest. Then, at the end of the flat top at T=1050 μs, the current density was small, which indicated that the time variation in the current-density distribution was related to that in the magnetic field distribution, as shown in Fig. 2.

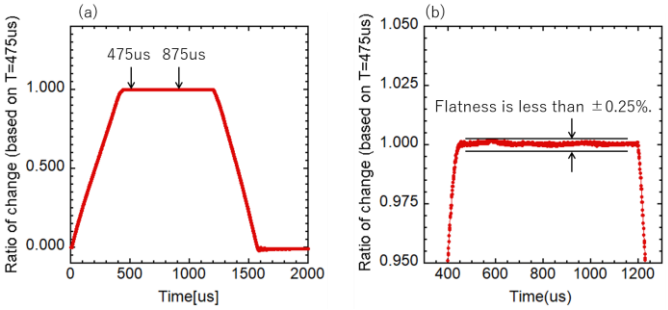

Fig. 4. Waveform of the excitation current used in the measurement. (a) Overall waveform. (b) Enlargement of the flat-top section. The output current is 4 kA because of the limitation in the experimental power supply, and the peak is set as one. The chopper-type switching power supply suppresses overshoot by adjusting the voltage pattern. Flat top flatness is less than ±0.25 %.

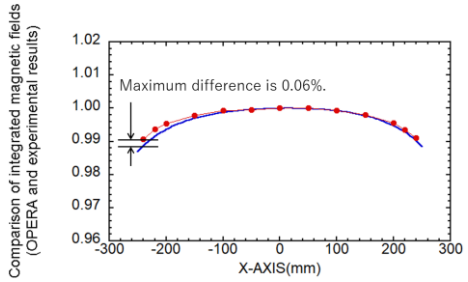

Fig. 5. Comparison of the (red dotted line) measurement and (blue solid line) analysis results of the integrated magnetic-field distribution using a long search coil. The width of the long search coil is 6 mm, the length is 3000 mm, and the number of coil turns is four. It is located at Y=0 mm. The largest deviation is 0.06 %, which very well agrees with the OPERA-3D results.

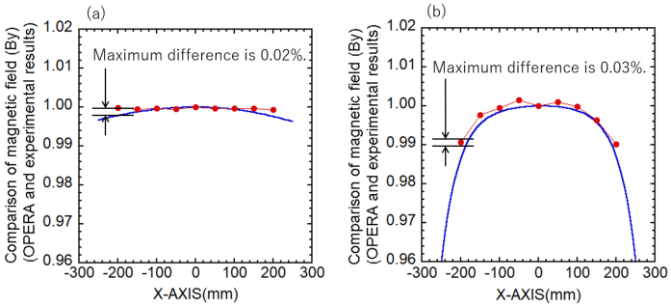

Fig. 6. Comparison of (red dotted line) measurement using a short search coil and (blue solid line) analysis results of the magnetic-field distribution at T=875 μs. The short search coil is 20 mm in diameter, contains 20 coil turns, and is located at Y=0 mm. (a) Center of the yoke. (b) Fringe region. The maximum deviation is the same as the one of the long search coil, which is small and in very good agreement.

This article has been accepted for publication in IEEE Transactions on Applied Superconductivity. This is the author's version which has not been fully edited and content may change prior to final publication. Citation information: DOI 10.1109/TASC.2022.3160152

B. *Comparison of the analysis and measurement results*

We evaluated the analysis results of OPERA-3D by comparing them with the measurement results. The power supply used for the measurement contained a pattern-adjustment function, which could suppress overshoot at the transient from a rising slope to the flat top of the current [9]. To obtain close to ideal flatness in the analysis model, we adjusted the flatness to less than ±0.25 %, which was the limit of the 600 kHz chopper method of this power supply.

The excitation waveform is shown in Fig. 4. The OPERA-3D analysis was performed at 16 kA rating of the actual power supply. However, in the experimental measurement, the excitation current was 4 kA because of the voltage limitation of the experimental power supply. For the magnetic field analysis between 4 and 16 kA using OPERA-3D, previous studies [5] and [7] confirmed the linear behavior and absence of saturation. The excitation waveform exhibited the same trapezoidal pattern, and the magnetic field at the center of the flat top T=875 μs was measured using the handmade short and long search coils of 0.1 mm wire [7]. The integrated magnetic field of a long search coil was used to evaluate the overall magnetic field, and a short search coil was used to evaluate the magnetic field distribution. The comparison result of the integrated magnetic field is shown in Fig. 5, and the magnetic field distribution is shown in Fig. 6. The maximum deviation between the analytical and measured results was less than 0.06 %, which confirmed agreement with that of OPERA-3D.

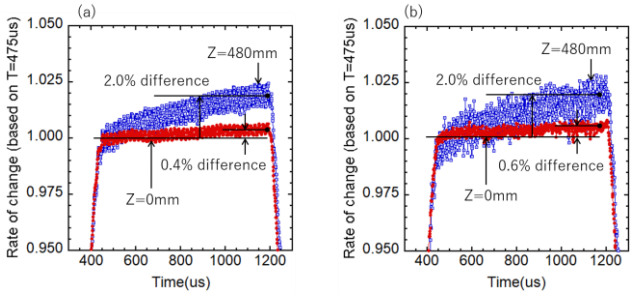

Fig. 7. Measurement results of the time variation in the magnetic field using a flux meter and a Hall probe. (a) Flux meter. (b) Hall probe. Uncertainties of the instruments were smaller than 0.2 %. The switching noises by the power supply influence the measuring probes equally whether they are located at the center or fringe. However, the magnetic-field at the fringe position is lower than that at the center position. Thus, errors of the normalized amplitude value appeared to be larger at the fringe. The amplitude difference at the same position indicates a noise-tolerance characteristic of the probes. The change in the center at Z=0 mm is small, whereas that in the fringe position at Z=480 mm is large.

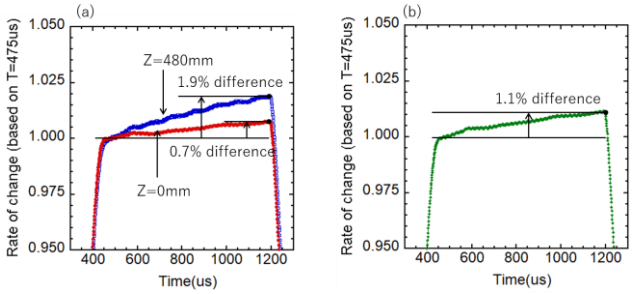

Fig. 8. Measurement results of the time variation in the magnetic field using short and long search coils. (a)Short search coil. (b)Long search coil. The change in the center at Z=0 mm is small, whereas that in the fringes at Z=480 mm is large. This trend is the same as those in the other probes. The long search coil is evaluated by integrating the distribution of the magnetic field on the Z axis from Z=-1500 mm to Z=+1500 mm; thus, the effect of fringing appears to be small.

C. *Measurement results of the pulsed magnetic field distribution using four different measuring instruments*

We tested the best probes to measure the bump magnet. The measurements were made using a Lake Shore Type 480 flux meter, a Type 475 Hall probe, and the short and the long search coils. The offset and common-mode noises in the search-coil measurements were eliminated [11], and the measured signals were then integrated to obtain the magnetic field.

To compare the analysis results with those of the OPERA-3D, we measured the time variation in the magnetic field at the center and the fringe positions of the yoke. The results are shown in Figs. 7 and 8. The measurements of all probes exhibited the same tendencies upon the magnetic field time variation as those of the OPERA-3D. The amplitude deviations of the magnetic field measured at the fringe positions of the flux meter and Hall probe were both 2.0 %. These measurements were larger than the analysis results of Fig.2(b). OPERA-3D includes the eddy current effect of the steel sheet in its calculations. The packing factor of the ratio of the steel plate thickness to the yoke length was set to 97%, and the conductivity of the electromagnetic steel plate was anisotropic with X=Y= 1.0E+7 S/m and Z=0. Further consideration will be needed to yield any findings about the difference of approximately 0.7 % between the analysis and the measurement.

D. *Probe pulse characteristics*

The characteristics of each probe were evaluated using Fast Fourier Transform (FFT) analysis, and we found that among the three tested probes, the short search coil could capture the frequency response of the experimental power supply. The analysis results are shown in Fig. 9. The fundamental switching frequency of the power supply is 50 kHz, and the composite frequency is 600 kHz with 12 multiplexes [12]. The FFT analysis results of the search coil verified the harmonics. The short search coil was used to check the spot magnetic field, and the long search coil was used to evaluate the effect on the

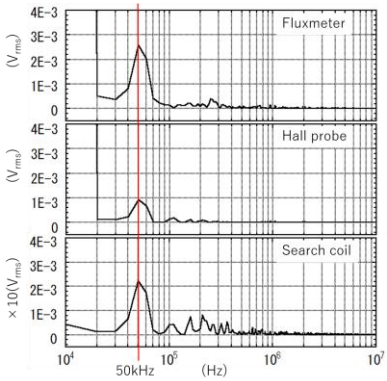

Fig. 9. Effective-value spectrum of the FFT analysis of the flux meter, Hall probe, and short search coil outputs at the flat-top center of the measured waveform. The graph shows a magnified view of the 50 kHz fundamental frequency of the switching power supply. The search coil best captures the harmonics. The flux meter has low harmonics due to the integration circuit. The Hall probes do not exhibit high frequency characteristics (50kHz).

This article has been accepted for publication in IEEE Transactions on Applied Superconductivity. This is the author's version which has not been fully edited and content may change prior to final publication. Citation information: DOI 10.1109/TASC.2022.3160152

whole beam. These two of search coil types were found to be suitable for fast pattern excitation of bump magnets and measurement of the time variation in magnetic field.

E. Probe-temperature characteristics

Fig. 10 shows the results of the time variation in the temperature and magnetic field distribution during 8 h of continuous operation. The peak current of 8 kA was used by applying the slower ramping rate of current, where rise and fall times were 800 μs, and the flat top time was 100 us (800-100-800) in a trapezoidal waveform at 25 Hz repetition. Each temperature was measured with a thermocouple [5]. The magnetic field strength was affected by the resistance and shape of changes in the coil due to the temperature increase. Only the Hall probe deviated by 0.4 %, which exceeded the specification value of ±0.015 %/°C for the temperature-drift compensation. Accurate measurement was not possible because of overheating of the Hall elements due to the eddy currents. The Hall probe is not suitable for pulse measurements.

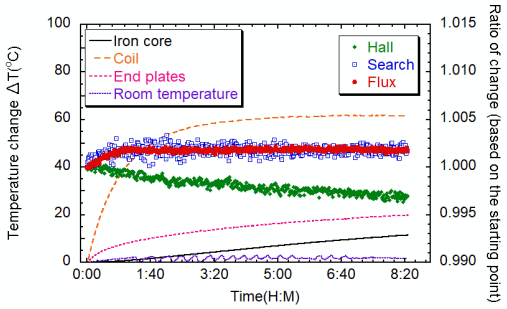

Fig. 10. Measurement results of the time variation in the electromagnet temperature and magnetic-field distribution during 8 h of continuous operation. As the temperature changes, the magnetic field strength also changes. Only the Hall probe significantly changes, showing a deviation of 0.4 %.

III. Temperature Evaluation of the Electromagnets

The temperature rise of the coil was fitted with the root-mean-square current (effective current), where the power dissipations in the coil are proportional to the square of the effective current. The effective-current of 1 kA corresponds to the 8 kA peak, and the coil temperature was measured every 0.25 kA. The effective-current of 2.6 kA corresponds to the maximum rated current of 16 kA in the waveform pattern for beam control. The temperature-measurement results and estimated values are shown in Fig. 11.

The cooling method of the new bump magnet did not have a water-cooled type due to the measures against leakage of activated water. The self-cooling temperature exceeded the temperature characteristic ΔT=200 °C of the Rika Lite IGL-T (Rika-Lite) insulation material of the coil [9],[13]. Air-cooling fans were fixed at the bottom of the coil outside the yoke and blew air from the bottom up. The fans were installed at four locations upstream and downstream of the beam-axis direction of the electromagnet. TYPE-A is an AC fan, and TYPE-B is a DC fan. The wind speed of TYPE-B was 9.3 m/s, which was approximately twice that of TYPE-A. The estimated coil temperature of the TYPE-B fan was 185 °C.

The analysis result using TEMPO [10] in OPERA-3D was 190 °C. Fig. 12 shows the coil model and results from the analysis. The measurement and the analysis results agreed with a high-accuracy temperature difference of 5 °C. The maximum temperature at the rated current was as expected, i.e., ΔT=200 °C even with the cooling. Satisfactory operating conditions could not be achieved with this test cooling system. However, the excitation current was assumed to be 12 kA for a 1-MW operating parameter using this new bump magnet. The effective-current at this time was 1.6 kA, and the coil temperature could be expected to be ΔT=75 °C. This temperature is within the acceptable range for long-term operation.

IV. Conclusion

We have confirmed that OPERA-3D, which performs dynamic magnetic field analysis, can design pulsed magnets with high accuracy by considering the effect of eddy currents. In addition, OPERA-3D can accurately evaluate the coil temperature of a pulsed magnet so that countermeasures against heat-generation problems can be designed. We also confirm that the search coil, which exhibits an excellent frequency response with less noise influence, can be used to investigate the time variation in the magnetic field and influence of the switching power supply.

Acknowledgment

The authors would like to thank Mr. Tanaka at Kyokuto Boeki Kaisha, Ltd. for his instruction and cooperation, and Prof. Y. Irie for his participation in the fruitful discussions and continuous support, and Prof. M. Yoshii for his support.

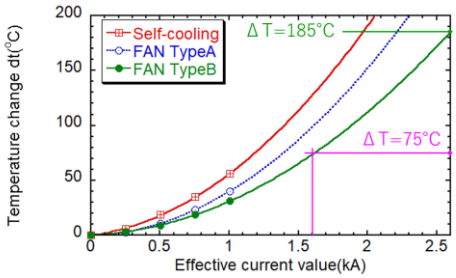

Fig. 11. Temperature measurement results of the coil and estimated rated value. Measurements are taken in three patterns: self-cooling, TYPE-A with AC fan, and TYPE-B with DC fan. The mark shows the measurement result, and the solid line shows the regression curve fitted to the square of the effective current.

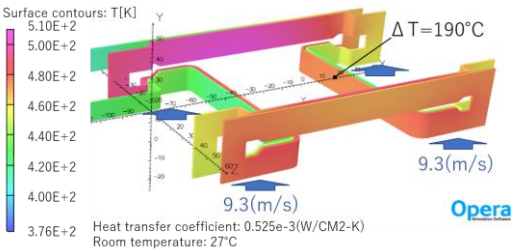

Fig. 12. Coil temperature analysis result at a rated current of 16 kA. Analysis is performed on the entire electromagnet. The effect of eddy currents on the electromagnet field is included. Only the coil is shown in the figure. Air-cooling fans are fixed at four locations upstream and downstream of the beam axis. The fans blow upward at a speed of 9.3 m/s from the bottom. The analytical temperature of the coil in the yoke at rated current is dt=190 °C.

REFERENCES

[1] J-PARC https://j-parc.jp/index-e.html

[2] K. Hasegawa, N. Hayashi, H. Oguri, K. Yamamoto, M. Kinsho, Y. Yamazaki, F. Naito, T. Koseki, N. Yamamoto, and M. Yoshii, "Performance and status of the J-PARC accelerators." *Proc. Int. Part. Accel. Conf.* 2018, pp.1038-1040.

[3] H. Hotchi, H. Harada, S. Kato, M. Kinsho, K. Okabe, P. K. Saha, Y. Shobuda, F. Tamura, N. Tani, Y. Watanabe, K. Yamamoto, and M. Yoshimoto, "Recent Progress of 1-MW Beam Tuning in the J-PARC 3-GeV RCS", *Proc. Int. Part. Accel. Conf.* 2016, pp.592-594.

[4] H. Hotchi,1 H. Harada, N. Hayashi, M. Kinsho, K. Okabe, P.K. Saha, Y. Shobuda, F. Tamura, K. Yamamoto, M. Yamamoto and M. Yoshimoto, "J-PARC 3-GeV RCS: 1-MW beam operation and beyond" *2020 IOP Publishing Ltd and Sissa Medialab*, https://doi.org/10.1088/1748-0221/15/07/P07022.

[5] T. Takayanagi, K. Yamamoto, J. Kamiya, P. K. Saha, T. Ueno, K. Horino, M. Kinsho, and Y. Irie, "A New Pulse Magnet for the RCS Injection Shift Bump Magnet at J-PARC." *IEEE Trans. Appl. Supercond.*, vol. 28, no. 3, Apr. 2018, no. 4100505.

[6] J. Kamiya, H. Kotoku, Y. Shobuda, T. Takayanagi, K. Yamamoto, T. Yanagibashi, K. Horino, "New Design of Vacuum Chambers for Radiation Shield Installation at Beam Injection Area of J-PARC RCS", *Proc. Int. Part. Accel. Conf.* 2019, pp.1255-1258.

[7] T. Takayanagi, K. Yamamoto, J. Kamiya, P. K. Saha, T. Ueno, K. Horino, M. Kinsho, and Y. Irie, "Comparative Studies of Three-Dimensional Analysis and Measurement for Establishing Pulse Electromagnet Design." *IEEE Trans. Appl. Supercond.*, Vol. 30, no. 4, Jun. 2020, no. 4901605.

[8] T. Takayanagi, J. Kamiya, M. Watanabe, T. Ueno, Y. Yamazaki, Y. Irie, J. Kishiro, I. Sakai, T. Kawakubo, S. Tounosu, Y. Chida, M. Watanabe, and T. Watanuki, "Design of the Shift Bump Magnets for the Beam Injection of the 3-GeV RCS in J-PARC." *IEEE Trans. Appl. Supercond.*, Vol. 16, no. 2, Jun. 2006, pp.1366-1369.

[9] T. Takayanagi, K. Kanazawa, T. Ueno, H. Someya, H. Harada, Y. Irie, M. Kinsho, Y. Yamazaki, M. Yoshimoto, J. Kamiya, M. Watanabe, and M. Kuramochi, "Measurement of the Paint Magnets for the Beam Painting Injection System in the J-PARC 3-GeV RCS." *IEEE Trans. Appl. Supercond.*, Vol. 18, no. 2, Jun. 2008, pp.310-313.

[10] OPERA-3D, ELEKTRA, TEMPO https://www.3ds.com/products-services/simulia/products/opera/

[11] T. Takayanagi, K. Kanazawa, T. Ueno, H. Someya, H. Harada, Y. Irie, M. Kinsho, Y. Yamazaki, M. Yoshimoto, J. Kamiya, M. Watanabe, M. Kuramochi, and K. Satou, "Improvement of the Shift Bump Magnetic field for a Closed Bump Orbit of the 3-GeV RCS in J-PARC." *IEEE Trans. Appl. Supercond.*, Vol. 28, no. 2, Jun. 2008, pp.306-309.

[12] T. Takayanagi, J. Kamiya, M. Watanabe, Y. Yamazaki, Y. Irie, M. Kishiro, I. Sakai, and T. Kawakubo, "Design of the Injection Bump System of the 3-GeV RCS in J-PARC." *IEEE Trans. Appl. Supercond.*, Vol. 16, no. 2, Jun. 2006, pp.1358-1361.

[13] Rika-Lite NIPPON RIKA KOGYOSHOCO., LTD., http://www.nippo-nrika.jp/en/